Csi-let-7a-5p delivered by extracellular vesicles from a liver fluke activates M1-like macrophages and exacerbates biliary injuries

Chao Yan[a,b,1,2], Qian-Yang Zhou[a,c,1], Jing Wu[a,d,1], Na Xu[a], Ying Du[a], Jing Li[a], Ji-Xin Liu[a], Stephane Koda[a], Bei-Bei Zhang[a,b], Qian Yu [a,b], Hui-Min Yang[a], Xiang-Yang Li[a,b], Bo Zhang[a,b], Yin-Hai Xu[e], Jia-Xu Chen[f,g], Zhongdao Wu[j,h,i], Xing-Quan Zhu[k], Ren-Xian Tang[a,b,2], and Kui-Yang Zheng[a,b,2]

[a]Jiangsu Key Laboratory of Immunity and Metabolism, Department of Pathogenic Biology and Immunology, Xuzhou Key Laboratory of Infection and Immunity, Xuzhou Medical University, Xuzhou 221004, People's Republic of China; [b]National Demonstration Center for Experimental Basic Medical Science Education, Xuzhou Medical University, Xuzhou 221004, People's Republic of China; [c]Department of Dermatology, Second Affiliated Hospital of Nanjing Medical University, Nanjing 210011, People's Republic of China; [d]Department of Chronic and Endemic Disease Control, Huai'an Center for Disease Control and Prevention, Huai'an 223001, People's Republic of China; [e]Department of Laboratory Medicine, Affiliated Hospital of Xuzhou Medical University, Xuzhou 221006, People's Republic of China; [f]National Institute of Parasitic Diseases, Chinese Center for Disease Control and Prevention, Chinese Center for Tropical Diseases Research, Shanghai 200025, People's Republic of China; [9]Key Laboratory of Parasite and Vector Biology, Ministry of Health, WHO Collaborating Center of Malaria, Schistosomiasis and Filariasis, Shanghai 200025, People's Republic of China; [h]Department of Parasitology, Zhongshan School of Medicine, Sun Yat-sen University, Guangzhou 510080, People's Republic of China; [i]Key Laboratory of Tropical Disease Control, Ministry of Education, Sun Yat-sen University, Guangzhou 510080, People's Republic of China; [j]Provincial Engineering Technology Research Center for Biological Vector Control, Sun Yat-sen University, Guangzhou 510080, People's Republic of China; and [k]College of Veterinary Medicine, Shanxi Agricultural University, Jinzhong 030801, People's Republic of China

Edited by Lora V. Hooper, University of Texas Southwestern Medical Center, Dallas, TX, and approved October 6, 2021 (received for review February 3, 2021)

Chronic infection with liver flukes (such as *Clonorchis sinensis*) can induce severe biliary injuries, which can cause cholangitis, biliary fibrosis, and even cholangiocarcinoma. The release of extracellular vesicles by *C. sinensis* (CsEVs) is of importance in the long-distance communication between the hosts and worms. However, the biological effects of EVs from liver fluke on biliary injuries and the underlying molecular mechanisms remain poorly characterized. In the present study, we found that CsEVs induced M1-like activation. In addition, the mice that were administrated with CsEVs showed severe biliary injuries associated with remarkable activation of M1-like macrophages. We further characterized the signatures of miRNAs packaged in CsEVs and identified a miRNA Csi-let-7a-5p, which was highly enriched. Further study showed that Csi-let-7a-5p facilitated the activation of M1-like macrophages by targeting *Socs1* and *Clec7a*; however, CsEVs with silencing Csi-let-7a-5p showed a decrease in proinflammatory responses and biliary injuries, which involved in the *Socs1*- and *Clec7a*-regulated NF-κB signaling pathway. Our study demonstrates that Csi-let-7a-5p delivered by CsEVs plays a critical role in the activation of M1-like macrophages and contributes to the biliary injuries by targeting the *Socs1*- and *Clec7a*-mediated NF-κB signaling pathway, which indicates a mechanism contributing to biliary injuries caused by fluke infection. However, molecules other than Csi-let-7a-5p from CsEVs that may also promote M1-like polarization and exacerbate biliary injuries are not excluded.

extracellular vesicles | Csi-let-7a-5p | biliary injuries | M1 macrophage | *Clonorchis sinensis*

The liver fluke *Clonorchis sinensis* (belongs to the family *Opisthorchiidae*) is widely prevalent in China, Korea, Vietnam, and the far eastern part of Russia, affecting about 35 million people (1, 2). The worm dwells in the bile duct and causes severe biliary injuries, which leads to cholangitis, periductal fibrosis, and cirrhosis in advanced cases (1). Furthermore, the incidence of cholangiocarcinoma (CCA) is closely associated with infection by such liver flukes throughout eastern Asia (3). However, the mechanisms underlying the liver fluke-driven chronic injuries are largely unknown (4).

During worm infection, severe biliary hyperplasias can be aroused with massive inflammation around the bile duct-so called ductular reactions (DRs) in the liver of infected animals and humans (5). Furthermore, DRs with the aberrant proliferation of cholangiocytes facilitate the development of intrahepatic biliary neoplasia in the condition of the inflammatory microenvironment (6). Among those regulators, the macrophage is the main role-player not only in fighting against worms and but also in the induction of hyperimmune responses by the secretion of various inflammatory mediators and cytokines, which can also lead to biliary hyperplasia in turn. It has been demonstrated that the activation of M1-like macrophages plays a critical role in the development of many cholangiopathies, such as primary biliary cirrhosis (PBC), primary sclerosing cholangitis (PSC), and biliary atresia (BA), as well as in worm infection conditions by the production of proinflammatory cytokines and reactive oxygen species (ROS)/nitric oxide synthase (NOS), which contributes to the pathogenesis of CCA (7, 8). However, the underlying molecular mechanisms by which *C. sinensis* activates M1 macrophages and conducts to DRs remain poorly understood.

Extracellular vesicles (EVs) are vesicular bodies secreted by living cells, which contain a large number of bioactive

Significance

Infection with liver flukes (such as *Clonorchis sinensis*) can induce severe biliary injuries. But we don't know how it happens. Here, we find that a microRNA Csi-let-7a-5p delivered by extracellular vesicles from *C. sinensis* is prone to M1-like activation of macrophages, thus leading to biliary proinflammatory responses and biliary injuries. These findings indicate a molecular mechanism contributing to biliary injuries caused by *C. sinensis*.

Author contributions: C.Y., R.-X.T., and K.-Y.Z. designed research; C.Y., Q.-Y.Z., J.W., and N.X. performed research; Q.-Y.Z., J.W., N.X., Y.D., J.L., J.-X.L., S.K., B.-B.Z., Q.Y., H.-M.Y., X.-Y.L., B.Z., Y.-H.X., J.-X.C., Z.W., and X.-Q.Z. contributed new reagents/analytic tools; C.Y., Q.-Y.Z., Y.D., R.-X.T., and K.-Y.Z. analyzed data; and C.Y. wrote the paper.

The authors declare no competing interest.

This article is a PNAS Direct Submission.

Published under the PNAS license.

[1]C.Y., Q.-Y.Z., and J.W. contributed equally to this work.

[2]To whom correspondence may be addressed. Email: yanchao6957@xzhmu.edu.cn, tangrenxian-t@163.com, or zky@xzhmu.edu.cn.

This article contains supporting information online at http://www.pnas.org/lookup/suppl/doi:10.1073/pnas.2102206118/-/DCSupplemental.

Published November 12, 2021.

substances such as nucleic acids, proteins, and lipids. EVs are important intercellular communicators involved in various biological processes and diseases (9). Emerging evidence demonstrates that EVs from helminthic excretory-secretory products (ESPs) are important mediators in the communication between the host and worms, which plays a critical role in the transmission of biological processes, regulation of immune response, mediating pathological damage, and survival (10–12). Among these components, extracellular miRNAs encapsulated and transferred by EVs are particularly of interest as they are stable and have the regulatory abilities by targeting multiple genes' expression at the posttranscriptional level in the recipient cells (13). *Schistosoma japonicum* EV miR-125 and bantam can promote the proliferation of macrophages and the production of tumor necrosis factor (TNF-α) by targeting *Pros1*, *Fam212b*, and *Clmp* gene expression (14). However, miRNA signatures in EVs from *C. sinensis* have not been investigated and the roles of these EV transferred miRNAs in modulating the immune responses of recipient cells, as well as in biliary hyperplasias, have not been elucidated.

In the present study, we investigated the roles of EVs from *C. sinensis* (CsEVs) in regulating the activation of macrophages and the contribution to biliary injuries; we further used next-generation sequencing to identify differential miRNA signatures in CsEVs from ESPs of *C. sinensis* and the adult of *C. sinensis*. We demonstrate that Csi-let-7a-5p enriched in CsEVs can promote activation of inflammatory macrophage by targeting at the *Clec7a*- and *Socs1*-mediated NF-κB signaling pathway, which may be involved in biliary hyperplasias. The findings of the present study provide a mechanism underlying worm–host interaction, which contributes to biliary injuries by infection with *C. sinensis*.

Materials and Methods

The study protocol was reviewed and approved by the Committee on Ethics of Animal Experiments, Xuzhou Medical University (201701w007). Animal experiments were strictly performed according to the Guidelines for Animal Experiments of Xuzhou Medical University and the National Guide for the Care and Use of Laboratory Animals.

Preparation of *C. sinensis* ESPs and CsEVs isolation were performed as described previously, with minor modification followed by zetaview nanoparticle tracking and transmission electron microscopy (TEM) (15–17). More details are provided in *SI Appendix*. Specific-pathogen-free C57BL/6J mice were used for animal study. More details regarding animal experiment are provided in *SI Appendix*. The RNAi assay was performed according to McVeigh et al. (18) and more details are provided in *SI Appendix*. Small RNA libraries of adult worms and CsEVs were conducted and these RNAs were sequenced, processed and analyzed by BGISEQ-500 sequencing technology at the Beijing Genomics Institute (BGI, Shenzhen, China). More details about RNA sequencing are provided in *SI Appendix*. Cell culture and transfection, dual-luciferase activity assay, ELISA, flow cytometry, qPCR, and Western blot were routinely performed. More detailed information about these assays are described in *SI Appendix*. Statistical analysis with more details, provided in *SI Appendix*, were performed with the use of the software package SPSS v19.0 (SPSS).

Results

Identification and Characterization of CsEVs. To obtain CsEVs, the adult worms were collected from the liver of experimentally infected guinea pigs and cultured in RPMI-1640 medium at 37 °C for 24 h after the worm bodies were completely washed. ESPs were subjected to serial centrifugation for the preparation of CsEVs, as shown in Fig. 1*A*. TEM showed that there were massive vesicles in the sediments and these EVs had a "typical" saucer-like shape with an average size of about 100 nm in diameter (Fig. 1*B*, red arrow). Nanoparticle tracking analysis confirmed that the majority of the microvesicles was 30∼150 nm with a peak at 100 to 120 nm in diameter (Fig. 1*C*). Upon quantification of CsEVs that we obtained, the concentration of CsEVs in our preparation was 272 particles per frame, which were equal to a concentration of 2.9×10^{11} particles per milliliter (Fig. 1*C*).

We also performed iodixanol-based density gradient centrifugation to compare with the CsEVs obtained by ultracentrifugation, as depicted in *SI Appendix*, Fig. S1*A*. We found that there were no obvious morphological differences between the CsEVs obtained by these two different methods (*SI Appendix*, Fig. S1 *B* and *C*).

CsEVs Induce Inflammatory (M1-Like) Macrophage Activation. As macrophages play critical roles in hepatic homeostasis and biliary diseases, we investigated the effects of CsEVs on macrophage function. First, to determine whether CsEVs can be specifically taken up by cells or not, CsEVs obtained by ultracentrifugation were specifically labeled with BODIPY TR Ceramide dye (red) and incubated with a macrophage cell line-RAW264.7 for 1 h. It was found that CsEVs were internalized by macrophages as shown by a microscope (Fig. 2*A*). Moreover, we further labeled CsEVs with carboxyfluorescein diacetate succinimidyl ester (CFSE) dye, which allows tracing CsEVs in the cells using flow cytometry. The fluorescent signal in bone marrow-derived macrophages (BMDMs) with CFSE-labeling CsEVs was increased, compared with those cells treated by no-labeled CsEVs (*SI Appendix*, Fig. S2 *A*, *Left*), indicating that CsEVs labeled by CFSE were also internalized by BMDMs. In addition, we also found that CsEVs labeled with CFSE were internalized by cultured hepatic stellate cells (*SI Appendix*, Fig. S2 *A*, *Right*), which suggested that CsEVs could be actively incorporated by macrophages.

To elucidate the effects of CsEVs on the macrophage function, the endotoxin in preparation of ESPs, CsEVs-free ESPs, and CsEVs were first detected using a commercial Limulus Amebocyte Lysate kit (Bioendo Technologies). The data showed that the concentrations of endotoxin in all these preparations were less than 0.05 EU/mL, indicating that the potential effects of endotoxin in these preparations on macrophages were trivial. Next, we evaluated pro- (M1-like) and anti-inflammatory (M2-like) markers in BMDMs that were stimulated by PBS, CsEVs (32 μg/mL), and worm cultures without CsEVs (CsEVs-free ESPs, 32 μg/mL) for 24 h. As shown in Fig. 2*B*, the flow cytometry data showed that CsEVs induced an increased expression of CD86 in $F4/80^{+}CD11b^{+}$ BMDMs after the treatment with CsEVs for 24 h, compared with those in the cells treated with PBS control or CsEVs-free ESPs (Fig. 2*B*) ($P < 0.05$). Furthermore, the data showed that the production of proinflammatory cytokines, including TNF-α and IL-6, were significantly increased in CsEVs-stimulated cells, compared with PBS control or CsEVs-free ESPs (Fig. 2 *C* and *D*) ($P < 0.01$). The levels of *Il1b* (encoding IL-1β) and *Nos2* (encoding iNOS) mRNA in CsEVs-stimulated cells were also remarkably higher than the medium control or CsEVs-free ESPs (Fig. 2 *E* and *F*, respectively) (more than 20 times, $P < 0.001$). However, compared with PBS, CsEVs decrease the levels of CD206 in $F4/80^{+}CD11b^{+}$ macrophages as shown by flow cytometry data (*SI Appendix*, Fig. S2*B*) ($P < 0.01$). In addition, the expression of M2-related *Arg1* (*SI Appendix*, Fig. S2*C*) ($P < 0.001$) and *Ym1* (*SI Appendix*, Fig. S2*D*) ($P < 0.001$) mRNA were decreased in BMDMs that were treated by CsEVs for 24 h, compared with medium control. Collectively, these data indicated that CsEVs induced proinflammatory macrophage activation, but tended to inhibit M2-like phenotype.

To exclude possible effects of CsEVs internalization, we isolated EVs from resting macrophages as irrelevant EVs for control. Compared with PBS, macrophages stimulated with irrelevant EVs cannot produce higher levels of IL-6 and TNF-α ($P > 0.05$), whereas CsEVs can stimulate macrophage to significantly increase the productions of IL-6 and TNF-α, compared with irrelevant EVs, suggesting that internalization of EVs has

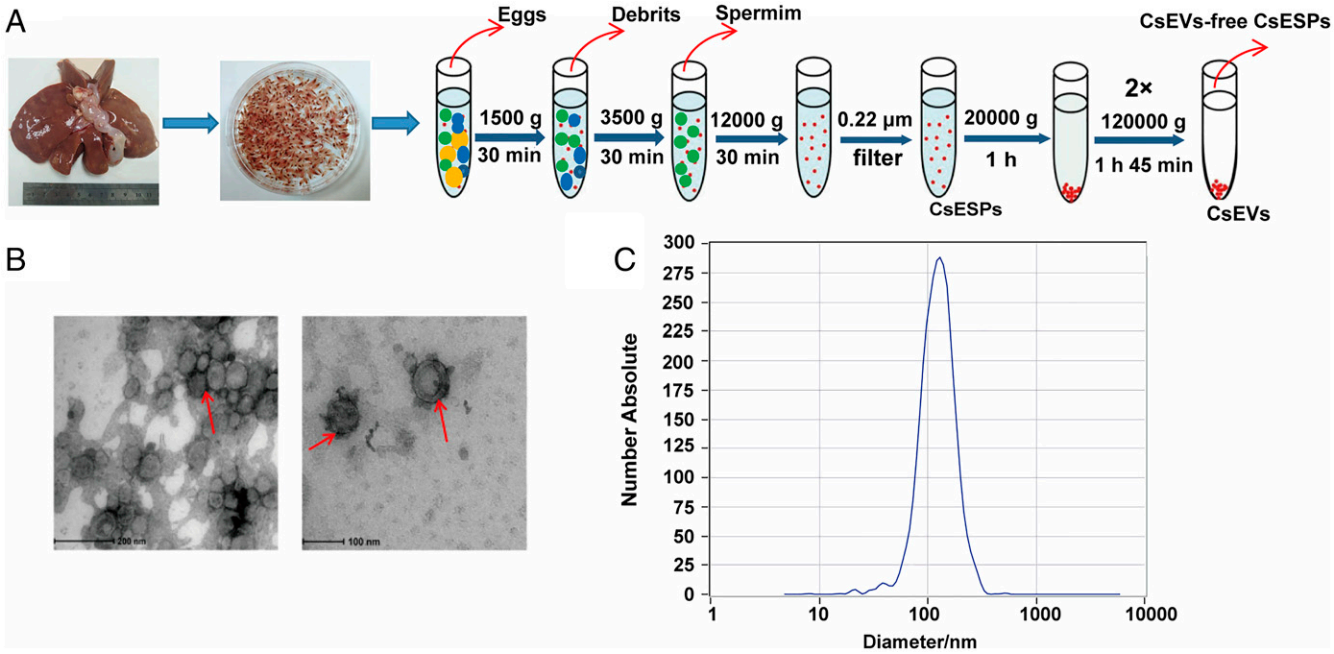

Fig. 1. Identification and characterization of EVs secreted by adults of *C. sinensis*. (*A*) Strategy of isolating CsEVs using differential centrifugation. (*B*) Morphology and structure of CsEVs released in culture medium by adult *C. sinensis* for 24 h were visualized by TEM (red arrow). (*C*) The size and distribution of CsEVs were determined using a nanoparticle tracking analysis (NTA).

no significant effects on the production of IL-6 and TNF-α by macrophages (*SI Appendix*, Fig. S3). Furthermore, CsEVs treated by RNase plus RIPA cannot stimulate macrophages to secret IL-6 as much as the ones stimulated by CsEVs without these treatments, but the production of IL-6 in macrophages stimulated by RNase plus RIPA-treated CsEVs were still higher than those of macrophages stimulated by irrelevant EVs (obtained from supernatant from resting macrophages) or PBS, suggesting that miRNAs delivered by the CsEVs may be critical to induce proinflammatory macrophages, although it cannot exclude that other molecules, such as proteins and lipids within CsEVs, may also promote activations of proinflammatory macrophages (*SI Appendix*, Fig. S3*B*) ($P < 0.001$).

CsEVs Promote Hepatic Inflammatory Macrophage Activation and Biliary Injuries. Because infection with *C. sinensis* causes severe biliary injuries, we hypothesized that CsEVs from *C. sinensis* may also lead to biliary injuries. To address this, the mice were intravenously injected with CsEVs or PBS at indicated time courses (Fig. 3*A*). The data showed that the serum indicators for biliary injuries, such as alkaline phosphatase (ALP), total bilirubin (TBIL), and total bile acid (TBA) were remarkably augmented due to intravenous injection of CsEVs, compared with the control group (Fig. 3 *B–D*). H&E staining showed that CsEVs altered biliary structures and induced massive inflammatory infiltration, as indicated by the Modified Hepatic Activity Index (mHAI) score (Fig. 3*E*) ($P < 0.001$). To further evaluate the biliary injuries, we evaluated the DR by the detection of DR marker CK19; the expression of CK19 was significantly increased, as shown by immunohistochemical (IHC) staining (Fig. 3*F*) ($P < 0.05$) after injection of CsEVs. For the evaluation of the proliferation of cholangiocytes, proliferation markers of Ki67 were also detected using IHC staining. It was found that the level of Ki67 was also increased in cholangiocyte-like cells in the liver of mice injected with CsEVs (Fig. 3*G*) ($P < 0.01$). These data suggest that CsEVs potently induce biliary injuries.

To investigate the effects of CsEVs on the function of hepatic macrophages in mice, we detected $CD68^+CD86^+$ (M1) and $CD68^+CD163^+$ (M2) macrophages using immunofluorescence assay. It was found that massive M1-like macrophages were significantly infiltrated around biliary ducts in CsEVs-injected mice (Fig. 3*H*) ($P < 0.001$). We also detected TNF-α–producing macrophages ($CD11b^+F4/80^+$) in the livers of these mice using flow cytometry; it was found that there was a significant increase of TNF-α–producing macrophages in the livers of CsEVs-treated mice, compared with the control group (Fig. 3*I*) ($P < 0.05$). Furthermore, the proinflammatory cytokines IL-6 and TNF-α in CsEVs-injected livers of mice were also significantly increased, compared with control mice (Fig. 3*J*) ($P < 0.001$). However, there were fewer M2 macrophages observed around the biliary ducts (*SI Appendix*, Fig. S2*E*). Together, these data indicate that CsEVs endow a hepatic proinflammatory environment to exacerbate biliary injuries.

To exclude possible effects of CsEVs internalization on the biliary injuries in vivo, we used the EVs from resting macrophages as irrelevant EVs (irrEVs) for control. Compared with irrEVs, CsEVs treatment can significantly induce biliary injuries as showed by ALP (*SI Appendix*, Fig. S4*A*) ($P < 0.01$), H&E staining using mHAI score (*SI Appendix*, Fig. S4*B*) ($P < 0.001$), and IHC staining of CK19 for indicating biliary proliferation (*SI Appendix*, Fig. S4*C*) ($P < 0.001$). However, there were no significant differences in biliary injuries between PBS-treated and irrEVs-treated mice (*SI Appendix*, Fig. S4) ($P > 0.05$).

Characterizations of miRNA Profiles in CsEVs. Since increasing data have demonstrated that the enriched-miRNAs can be delivered by EVs, we first examined whether these miRNAs could be incorporated by macrophages or not; miRNAs within CsEVs were labeled by membrane-permeant RNA specific dye-(SYTO RNASelect, Life Technologies) and incubated with macrophages for 1 h. CsEVs labeled with the dye were found within the macrophages as shown by the fluorescence

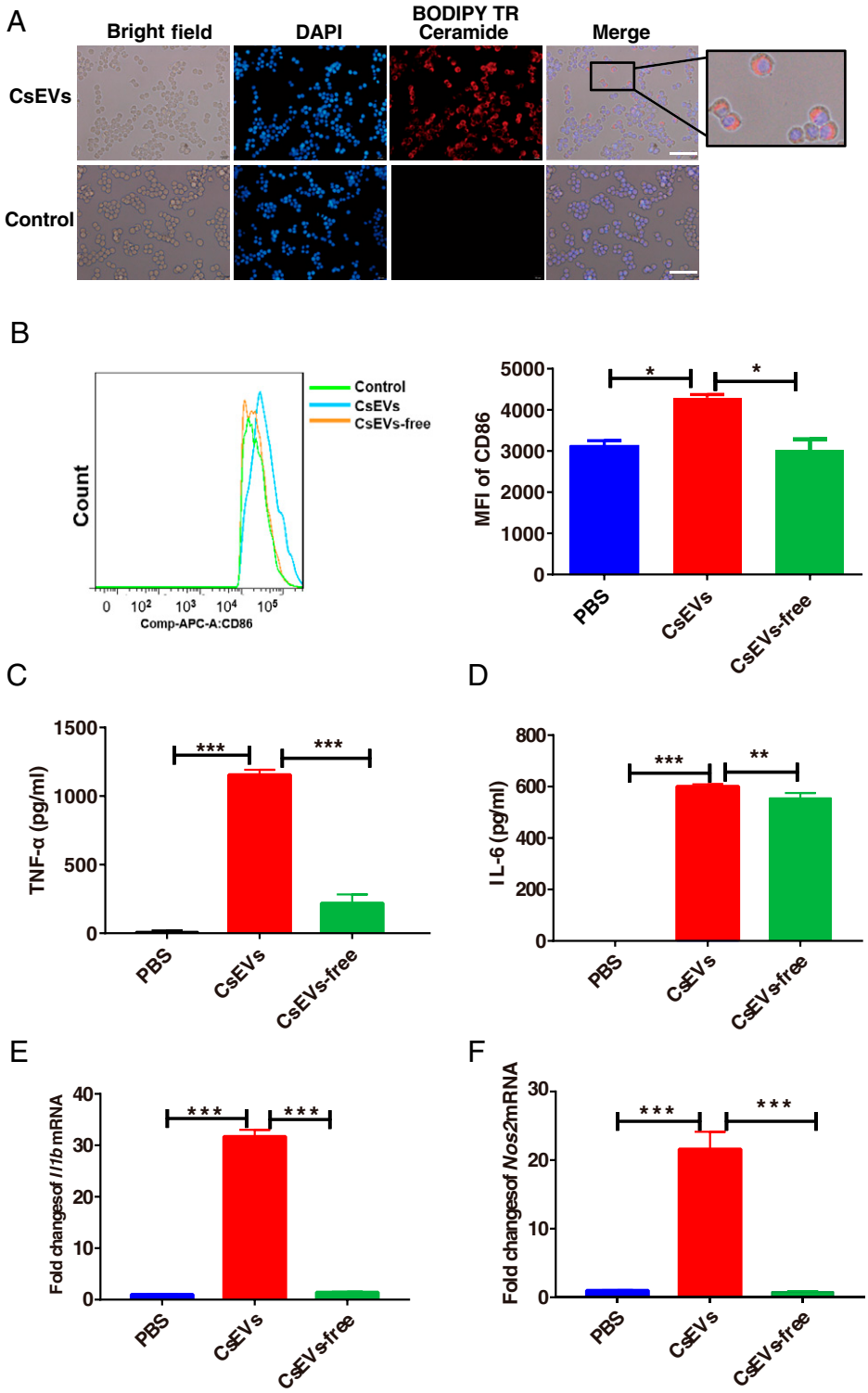

Fig. 2. CsEVs induce the activation of M1-like macrophages. (*A*) The red dye-labeled CsEVs were internalized by RAW 264.7 after treatment for 12 h. (Scale bars, 50 μm.) (*B*) The expression of CD86 in F4/80^{+}CD11b^{+} BMDMs after treatment with PBS, CsEVs (32 μg/mL), or CsEVs-free (32 μg/mL) for 24 h. (*C* and *D*) The secretions of TNF-α (*C*) and IL-6 (*D*) produced by the BMDMs after treatment with PBS, CsEVs (32 μg/mL), or CsEVs-free (32 μg/mL) for 24 h as determined by ELISA. (*E* and *F*) The relative expression of *Il1b* (encoding IL-1β) and *Nos2* (encoding iNOS) in the BMDMs after treatment with PBS, CsEVs (32 μg/mL) or CsEVs-free (32 μg/mL) for 24 h as determined by qPCR. The values were expressed as mean ± SEM. Compared with indicated groups, *$P < 0.05$, **$P < 0.01$, ***$P < 0.001$.

microscope (Fig. 4*A*). To elucidate the mechanisms by which CsEVs with proinflammatory properties aggravate biliary injuries, we further analyzed the miRNA expression profiles in CsEVs as well as in parental worm bodies using the high-throughput sequencing. All the raw data of two small RNA sequencing were deposited in the database of Gene Expression Omnibus (GEO) in the National Center for Biotechnology Information (NCBI) (accession no. GSE137695). The

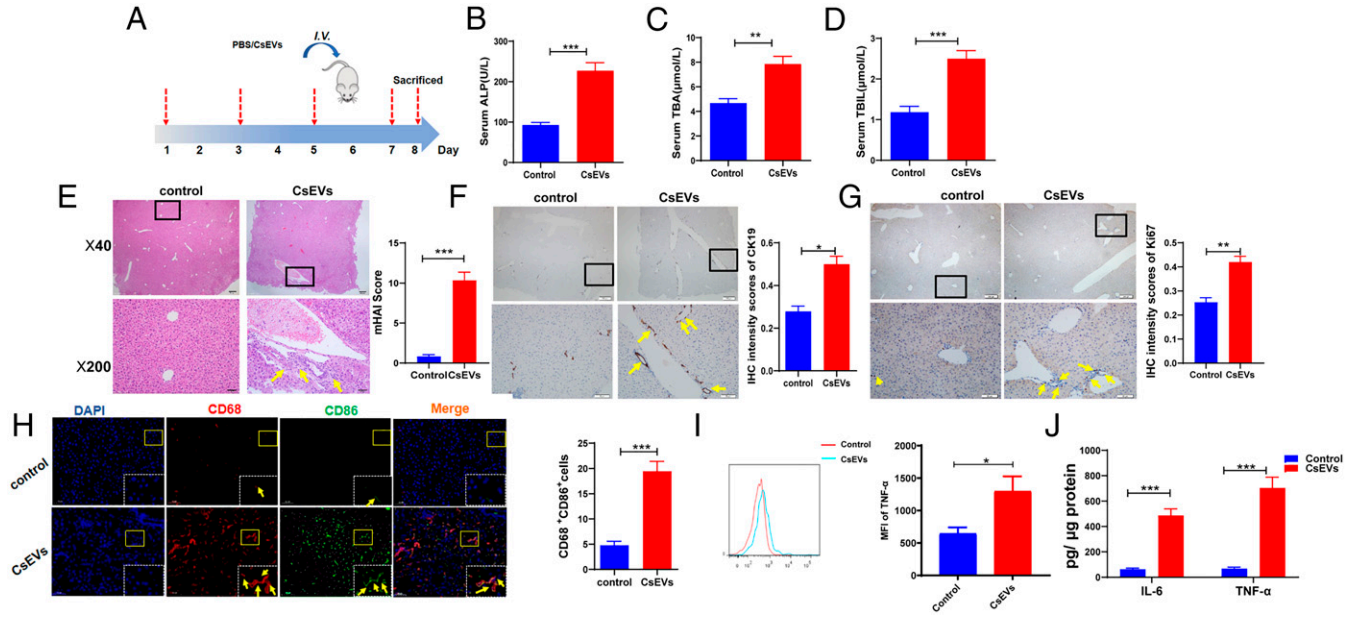

Fig. 3. CsEVs cause severe biliary injuries. (*A*) The study design. The mice that were intravenously injected with CsEVs (0.5 mg/mL, ~100 μL) or PBS (100 μL) at the indicated time. (*B–D*) The levels of serum indicators for biliary injuries, such as ALP (*B*), TBA (*C*), and TBIL (*D*) in the mice treated by CsEVs or PBS. (*E*) H&E staining showing histological changes (*Left*) was evaluated using mHAI scoring (*Right*) in the liver of mice treated with CsEVs or PBS; yellow arrows showed infiltered immune cells. (*F*) The expression of CK19 (yellow arrows) in the liver of mice treated with CsEVs or PBS by IHC staining. (*G*) The expression of Ki67 (yellow arrows) in the liver of mice treated with CsEVs or PBS by IHC staining. (*H*) The proportion of $CD86^+CD68^+$macrophages (M1-like, yellow arrows) in the livers of mice that were hydrodynamically injected with CsEVs or PBS as determined by immunofluorescence assay. (*I*) TNF-α–producing macrophages ($CD11b^+F4/80^+$) in livers of these mice were detected using flow cytometry. (*J*) The levels of IL-6 and TNF-α in the livers of mice were determined by ELISA. The values were expressed as mean ± SEM. Compared with indicated groups, $*P < 0.05$, $**P < 0.01$, $***P < 0.001$.

sequencing data showed that some miRNAs were highly detected in CsEVs (Fig. 4*B*). Furthermore, a heatmap showed that some miRNAs—such as Csi-let-7a-5p, Csi-miR-61-3p, Csi-miR-1b-3p, and Csi-miR-71a-5p—were highly enriched in CsEVs when compared with the abundance of these miRNAs in the adult worms (Fig. 4*C*). Among these miRNAs, Csi-let-7a-5p was one of the most enriched in the CsEVs, compared with the transcripts per kilobase per million (TPM) values of Csi-let-7a-5p in adult worms (Fig. 4*C*). qPCR data also showed that the relative level of Csi-let-7a-5p in CsEVs was 20 times higher than that in the adult worms, which confirmed the sequencing data indicating that Csi-let-7a-5p was highly enriched in CsEVs (Fig. 4*D*) ($P < 0.001$).

Csi-let-7a-5p Binds with *Socs1* and *Clec7a* to Promote the Activation of M1-Like Macrophage. According to the sequencing data, the potential targets of Csi-let-7a-5p were predicted using the intersection of TargetScan, MiRanda, and PicTar databases. According to the bioinformatic analysis above, the genes of *Socs1* and *Clec7a* were identified as the potential targets of Csi-let-7a-5p (Fig. 4*E*). As it has been determined that *Socs1* is one of the targets of let-7a-5p using luciferase reporter assay (19), we further investigated whether Csi-let-7a-5p inhibited the expression of *Clec7a* by binding to the region of *Clec7a* 3′UTR or not. The cells were transfected with either a pmiReport empty vector control, *Clec7a*-3′UTR (full-length, WT), or deletion of Csi-let-7a-5p binding site on *Clec7a* 3′UTR (MUT) report gene plasmid (Fig. 4*F*). The activity of luciferase in the WT group was significantly lower than that in the MUT group (Fig. 4*F*) ($P < 0.01$). However, the activity of the reporter gene after deletion remained unchanged, compared with the control plasmid group (Fig. 4*F*) ($P > 0.05$). These findings suggested that Csi-let-7a-5p could only bind *Clec7a* 3′UTR without the deletion (Fig. 4*F*).

In our study, we found a significant decrease in the levels of SOCS1 and Dectin-1 (encoded by *Clec7a*) while the level of P-p65 was remarkably increased after the stimulation of the macrophages (*SI Appendix*, Fig. S5*A*) ($P < 0.05$) or mice (*SI Appendix*, Fig. S5*B*) ($P < 0.05$) with CsEVs. To further determine whether Csi-let-7a-5p can inhibit the expression of SOCS1 and Dectin-1 in macrophages or not, we transfected Csi-let-7a-5p mimic or its scramble control into RAW264.7 cells for 24 h, then the total RNA and protein from these cells were extracted to detect the expression of these targets using qPCR and Western blot, respectively. It was found that Csi-let-7a-5p mimic were successfully transfected into the receipt cells (about 200 times higher than that of the control group, $P < 0.001$) (Fig. 4*G*). Furthermore, overexpression of Csi-let-7a-5p could significantly inhibit the mRNA expression of *Socs1* and *Clec7a* (Fig. 4*H*) ($P < 0.01$). Similarly, it was confirmed that both SOCS1 and Dectin-1 were suppressed by the overloaded Csi-let-7a-5p in macrophages at the protein level (Fig. 4*I*) ($P < 0.05$). These results confirmed that Csi-let-7a-5p could bind with *Clec7a* or *Socs1* 3-′UTR directly to inhibit their expression.

To investigate the roles of Csi-let-7a-5p in the activation of macrophages, we also detected M1/M2-relative makers after the macrophages were treated with Csi-let-7a-5p mimic or scramble control for 24 h. Compared with a scrambled control, it showed that overexpression of Csi-let-7a-5p significantly induced M1 markers gene expression (*Il6*, *Tnfa*, *Il1b*, and *Nos2*; $P < 0.01$) (Fig. 4*J*), as well as the production of IL-6 and TNF-α cytokines (Fig. 4*K*) ($P < 0.05$); however, it also tended to decrease the levels of M2 markers' (*Ym1* and *Arg1*) gene expression (*SI Appendix*, Fig. S6*A*) ($P < 0.05$). Furthermore, we detected CD86 or CD206 expression in macrophages using flow cytometry. It was found that the mean fluorescence intensity (MFI) of CD86 in Csi-let-7a-5p mimic-treated cells were significantly increased compared with the cells that were treated with scrambled control

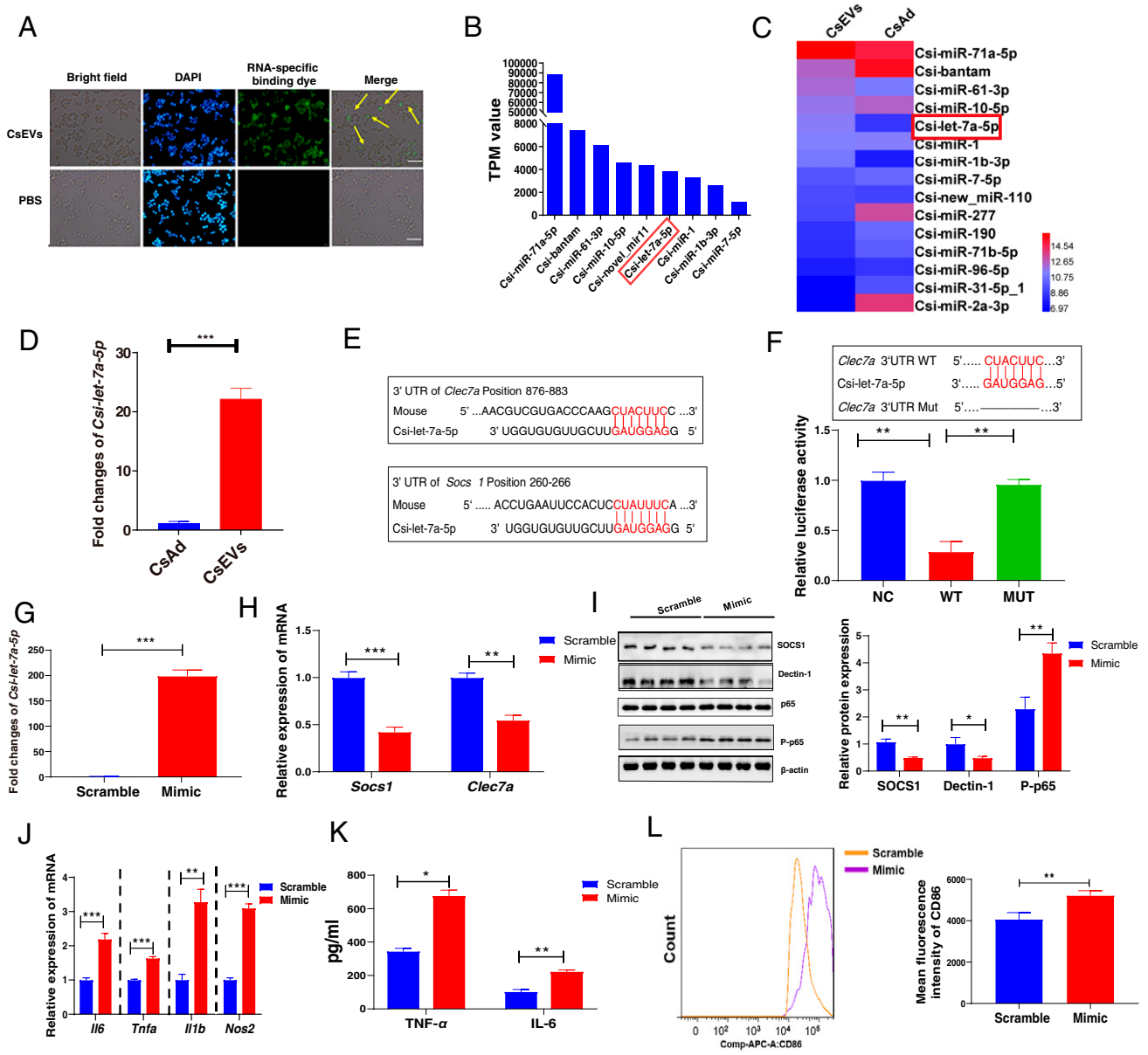

Fig. 4. Characterization of enriched miRNAs profiles in CsEVs and identification of the targets of Csi-let-7a-5p packaged by CsEVs. (*A*) CsEVs delivering miRNAs labeled with the green dyes were found within the macrophages as shown by the fluorescence microscope (scale bars, 50 μm). The yellow arrow shows the internalized miRNA in the macrophage cell line RAW 264.7. (*B*) The top nine most abundant miRNAs (>1,000 TPM values) in CsEVs were identified using high-throughput sequencing. (*C*) The comparison of the abundances of miRNAs (>100 TPM) between CsEVs and adult worms showed by the heatmap. (*D*) The relative expression of Csi-let-7a-5p in the CsEVs and adult worms were determined by qPCR. (*E*) The potential binding sites of Csi-let-7a-5p in 3′UTR of *Clec7a* and *Socs1* were predicted using the intersection of TargetScan, MiRanda, and PicTar databases. (*F*) The luciferase activities were measured in the 293T cells that were transfected with either a pmiReport empty vector control (NC), *Clec7a*-3′UTR (full length, WT), or deletion of Csi-let-7a-5p binding site on *Clec7a* 3′UTR (MUT) report gene plasmid for 24 h. (*G*) The levels of Csi-let-7a-5p in macrophages after Csi-let-7a-5p mimic were transfected for 24 h using qPCR. (*H*) The relative mRNA expression of *Socs1* and *Clec7a* in the macrophages that were transfected with Csi-let-7a-5p mimic or scramble for 24 h. (*I*) The levels of SOCS1, Dectin-1 (encoded by *Clec7a*), and P-p65 in macrophages that were transfected with Csi-let-7a-5p mimic or scramble for 24 h. (*J*) The relative mRNA expression of *Il6*, *Tnfa*, *Il1b,* and *Nos2* in the macrophage that was transfected with Csi-let-7a-5p mimic or scramble for 24 h. (*K*) The secretion of TNF-α and IL-6 in the cultures of macrophages that were transfected with Csi-let-7a-5p mimic or scramble for 24 h. (*L*) The mean fluorescence intensity of CD86 in macrophages that were transfected with Csi-let-7a-5p mimic or scramble for 24 h using flow cytometry. The values were expressed as mean ± SEM. Compared with indicated groups, **P* < 0.05, ***P* < 0.01, ****P* < 0.001.

(Fig. 4*L*) ($P < 0.01$), but the expression of CD206 in macrophages that were stimulated with Csi-let-7a-5p mimic was lower than that in cells that were treated with scrambled control (*SI Appendix*, Fig. S6*B*). As the NF-κB signaling pathway is critical in the secretion of proinflammatory cytokines (e.g., IL-6 and TNF-α), which are negatively regulated by SOCS1 (20), we also found that the level of the P-p65, the subunit of NF-κB, was significantly increased when the cells were transfected with Csi-let-7a-5p mimic, compared with scrambled control (Fig. 4*I*) ($P < 0.01$). Taken together, these findings demonstrate that Csi-let-7a-5p promotes an M1-like macrophages by targeting *Clec7a* and *Socs1* via the NF-κB signaling pathway.

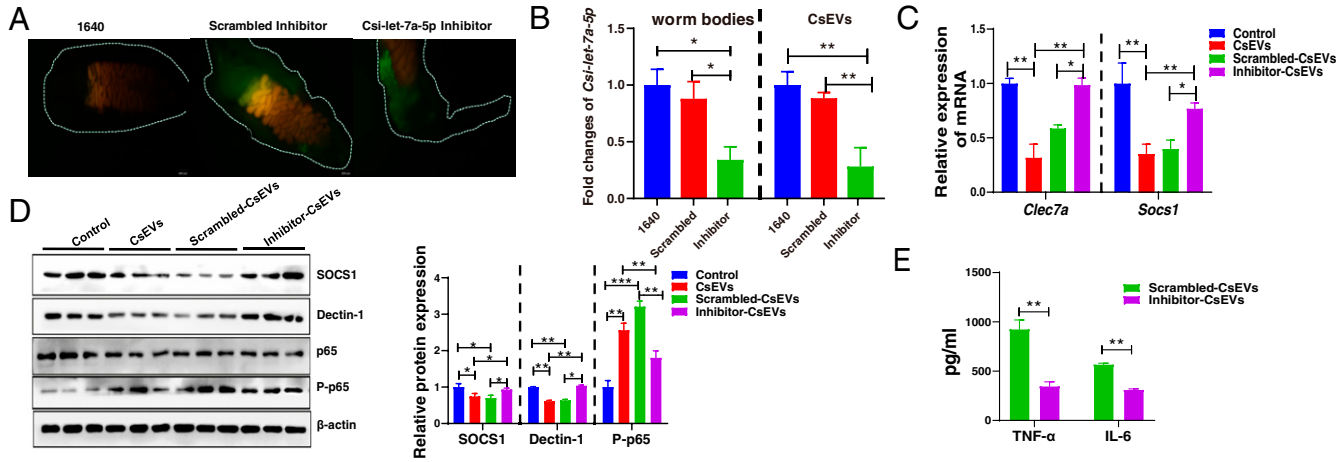

Fig. 5. Knockdown of Csi-let-7a-5p decreased inflammatory responses in macrophages by the SOCS1 and Dectin-1–mediated NF-κB signaling pathway. (*A*) Csi-let-7a-5p specific siRNA oligonucleotide or scrambled siRNA labeled with a green dye were observed within worm bodies. (*B*) The relative expression of mature Csi-let-7a-5p in the Csi-let-7a-5p-siRNA (inhibitor), scrambled siRNA, or 1640-treated worms (*Left*). CsEVs from these different treated worms were prepared as described in Fig. 1*A*; the relative expression of mature Csi-let-7a-5p in CsEVs (from 1640-treated worms), scrambled-CsEVs (from scrambled siRNA-treated worms), and inhibitor-CsEVs (from Csi-let-7a-5p-siRNA–treated worms) were determined by qPCR. (*C*) The relative expression of *Socs1* and *Clec7a* in macrophages that were stimulated by inhibitor-CsEVs, scrambled-CsEVs, CsEVs, or PBS for 24 has been determined by qPCR. (*D*) Western-blot showed the protein levels of SOCS1, Dectin-1, and P-p65 in macrophages that were stimulated by PBS, CsEVs, scrambled-CsEVs, or inhibitor-CsEVs for 24 h. (*E*) The secretion of IL-6 and TNF-α in the cultures of macrophages that were stimulated by scrambled-CsEVs or inhibitor-CsEVs for 24 h as determined by ELISA. The values were expressed as mean ± SEM. Compared with indicated groups, $*P < 0.05$, $**P < 0.01$, $***P < 0.001$.

Inhibition of Csi-let-7a-5p in CsEVs Decreased Inflammatory Responses in Macrophage by Targeting at SOCS1 and Dectin-1. To further elucidate the roles of Csi-let-7a-5p in the activation of proinflammatory macrophages, Csi-let-7a-5p in adult worms was knocked down using short-interfering RNA (siRNA) technology. To confirm this, Csi-let-7a-5p specific siRNA or scrambled siRNA labeled by green dye were observed within the worm bodies (Fig. 5*A*), and qPCR data showed that the level of mature Csi-let-7a-5p in the adult worm bodies soaked with Csi-let-7a-5p–specific siRNA oligonucleotide was significantly reduced, compared with medium-treated worms or scrambled oligonucleotide-treated worms (~70% reduction, $P < 0.05$) (Fig. 5 *B*, *Left*). To exclude the side-effects of RNAi reagents on the survival, behaviors, and reproduction of worms, which may induce the decrease of Csi-let-7a-5p, we observed the survival of worms, the amount of the eggs and ultrastructure of eggs produced from Csi-let-7a-5p-siRNA (inhibitor), scrambled siRNA, or 1640-treated worms during the whole experiment. The data showed that there were no significant differences in the survival rates, the amounts of the eggs, and the ultrastructure of eggs of worms between Csi-let-7a-5p-siRNA/scramble control-treated and normal cultured worms (*SI Appendix*, Fig. S7 *A–C*) ($P > 0.05$). We further collected ESPs from Csi-let-7a-5p-siRNA (inhibitor), scrambled siRNA, or medium-treated worms (cultured for 24 h) for preparation of CsEVs (namely inhibitor-CsEVs, scrambled-CsEVs, and CsEVs, accordingly).

First, to check the morphologic changes of CsEVs from these different worms using TEM, it was found that there were no obvious morphologic changes in CsEVs between scramble-treated worms and siRNA-treated worms (*SI Appendix*, Fig. S7*D*). We also evaluated whether Csi-let-7a-5p in CsEVs from siRNA oligonucleotide-treated worms were also silenced or not; we found that the levels of Csi-let-7a-5p were significantly decreased in inhibitor-CsEVs (~70% decreased compared with scrambled-CsEVs or CsEVs; $P < 0.01$) (Fig. 5 *B*, *Right*). These data suggested that Csi-let-7a-5p in CsEVs was also successfully silenced using Csi-let-7a-5p–specific siRNA. These CsEVs were further employed to incubate with macrophages for 24 h. It was found that the decreased levels of *Clec7a* and *Socs1* mRNA were significantly reversed after Csi-let-7a-5p was inhibited in CsEVs (Fig. 5*C*) ($P < 0.05$). Furthermore, Western blot assay showed that the protein levels of Dectin-1 and SOCS1 were also increased in inhibitor CsEVs-treated macrophages, compared with scrambled-CsEVs (Fig. 5*D*) ($P < 0.05$). Besides, the proinflammatory activation of macrophages induced by CsEVs was significantly attenuated by Csi-let-7a-5p–inhibited CsEVs as shown by the decreased levels of IL-6 and TNF-α protein (Fig. 5*E*) ($P < 0.01$). We also found that the level of P-p65 of NF-κB was significantly decreased in cells that were stimulated by Csi-let-7a-5p–inhibited CsEVs, compared with those in scrambled-CsEVs-treated macrophages (Fig. 5*D*) ($P < 0.01$). However, Csi-let-5p–inhibited CsEVs trended to increase *Arg1* and *Ym1* mRNA produced by macrophages, compared with scrambled-CsEVs macrophages (*SI Appendix*, Fig. S7*E*) ($P < 0.01$). Collectively, inhibition of Csi-let-7a-5p in CsEVs decreased the activation of M1-like macrophages by targeting SOCS1 and Dectin-1–mediated NF-κB signaling pathway.

Inhibition of Csi-let-7a-5p in CsEVs Reverses the Biliary Injuries and Hepatic Inflammatory Responses. To further investigate whether knockdown of Csi-let-7a-5p in CsEVs ameliorated biliary injuries or not, the mice were intravenously injected with scrambled-CsEVs or inhibitor-CsEVs (Fig. 6*A*). It was found that CsEVs with knocked-down Csi-let-7a-5p improved the index of liver weight/body weight of mice (Fig. 6*B*) ($P < 0.05$). We also evaluated the biliary injuries indicated by the liver biochemistry markers—such as serum ALP, TBIL and TBA in mice and the biochemical analysis showed that the levels of these indicators in the sera of mice treated with inhibitor-CsEVs were significantly decreased, compared with those mice injected with scrambled-CsEVs (Fig. 6*C*) ($P < 0.05$), indicating that inhibition of Csi-let-7a-5p in CsEVs ameliorated biliary damages. To confirm this, we further evaluated the histopathological changes and infiltrations of inflammatory cells in the liver of mice using HE staining; it showed that the damaged biliary structures and infiltrated inflammatory cells in the livers of inhibitor-CsEVs-

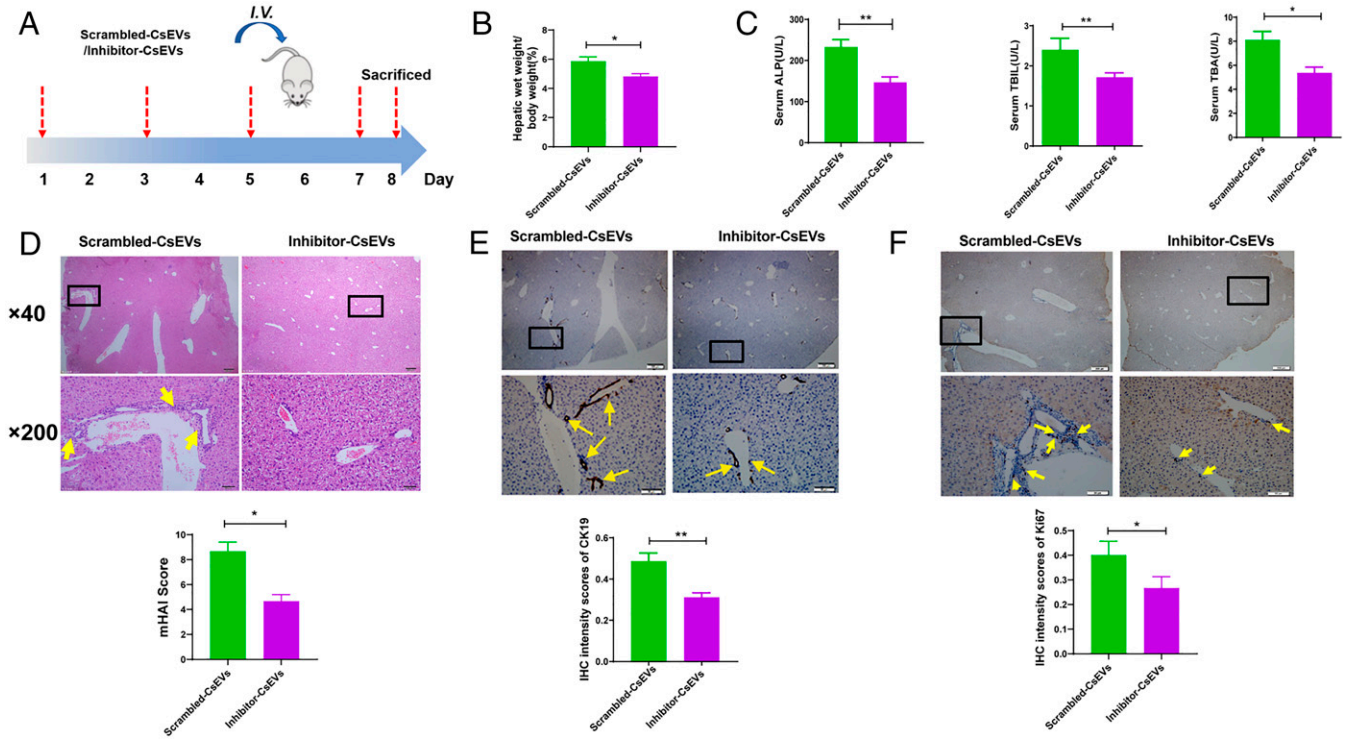

Fig. 6. Gene-silencing of Csi-let-7a-5p in CsEVs ameliorates the biliary injuries. (*A*) The study design. The mice that were injected with scrambled-CsEVs (0.5 mg/mL, ~100 μL) or inhibitor-CsEVs (0.5 mg/mL, ~100 μL) at the indicated time courses. (*B*) The ratio of liver weight to body weight of mice (%). (*C*) The levels of serum indicators for biliary damages caused by scrambled-CsEVs or inhibitor-CsEVs; (*D*) Histological changes of livers from the mice administrated with scrambled-CsEVs or inhibitor-CsEVs were indicated by mHAI scores. The infiltrations of inflammatory cells in these mice are indicated by yellow arrows. (*E* and *F*) Ductal reactions were evaluated using the expression of CK19 (*E*) and Ki67 (*F*) as shown by IHC staining (yellow arrows). The values were expressed as mean ± SEM. Compared with indicated groups, $*P < 0.05$, $**P < 0.01$.

treated mice were ameliorated, compared with those treated with scrambled-CsEVs (Fig. 6*D*) (as shown by mHAI scores, $P < 0.05$). The data of IHC staining for CK19 and Ki67 indicating DRs also suggested that DRs were decreased in the liver of inhibitor-CsEVs-treated mice, compared with mice that were administrated by scrambled-CsEVs (Fig. 6*E* for CK19 staining; Fig. 6*F* for Ki67 staining) ($P < 0.05$).

We also evaluated the hepatic immune responses in the mice after administration of scrambled CsEVs or inhibitor-CsEVs. The immunofluorescent staining showed that the proportion of M1-like ($CD68^+CD86^+$) macrophages was remarkably decreased after the mice were treated with the inhibitor-CsEVs, compared with scrambled-CsEVs-treated mice (Fig. 7*A*) ($P < 0.01$). However, the inhibitor-CsEVs did not alter the proportion of M2-like macrophages ($CD68^+CD163^+$) in the livers of mice, compared with scrambled-CsEVs mice (*SI Appendix*, Fig. S8*A*) ($P > 0.05$). We also detected proinflammatory or antiinflammatory cytokines using ELISA or qPCR. The levels of secreted IL-6 and TNF-α cytokines in the livers of inhibitor-CsEVs-treated mice were significantly lower than those in the mice administrated with scrambled-CsEVs (Fig. 7*B*) ($P < 0.05$). Furthermore, the levels of *Tnfa*, *Il6*, *Il1b*, and *Nos2* mRNA in the livers of inhibitor-CsEVs-treated mice were significantly decreased, compared with those mice that were administrated by scrambled-CsEVs (Fig. 7*C*) ($P < 0.05$). But we did not find any changes in the levels of neither *Ym1* nor *Arg1* between inhibitor-CsEVs-treated mice and scrambled-CsEVs-treated mice (*SI Appendix*, Fig. S8*B*) ($P > 0.05$). To check the signaling pathway that Csi-let-7a-5p targeted, we detected the levels of SOCS1, Dectin-1, and P-p65 in the livers of the mice that were treated by PBS, CsEVs, scrambled-CsEVs or inhibitor-CsEVs. It was found that the levels of SOCS1 and Dectin-1 in the CsEVs-treated mice were remarkably lower than those in PBS-treated mice; but the expression of SOCS1 and Dectin-1 were significantly increased in the mice treated with inhibitor-CsEVs, compared with those in scrambled-CsEVs-treated mice (Fig. 7*D* for mRNA level, $P < 0.01$; Fig. 7*E* for protein level, $P < 0.05$). Accordingly, the level of phosphorylated p65 in the liver of CsEVs-treated mice was significantly higher than that in those mice administrated with PBS while it was significantly decreased in the liver of inhibitor-CsEVs-treated mice, compared with those mice administrated with scrambled-CsEVs (Fig. 7*E*) ($P < 0.05$). Taken together, these data suggested that knockdown of Csi-let-7a-5p in CsEVs relieved the biliary inflammation and thus ameliorated biliary injuries.

Discussion

Chronic infection with *C. sinensis* and *Opisthorchis viverrini* can cause biliary injuries that are considered as a principal risk factor of CCA in the liver flukes-endemic regions, although the mechanisms that are responsible for biliary damage are largely unknown (3). In our present study, we characterized EVs from *C. sinensis* and found that CsEVs induced the activation of macrophages to M1-like phenotype and promoted biliary injuries. Furthermore, a miRNA Csi-let-7a-5p enriched in CsEVs was identified, which preferred the activation of proinflammatory macrophages and facilitated biliary injuries by targeting at the *Clec7a*- and *Socs1*-modulated NF-κB signaling pathway (Fig. 8).

It has been suggested that helminth-derived EVs facilitate long-distance communication between host cells and worms by delivering many bioactive molecules, such as miRNAs, proteins,

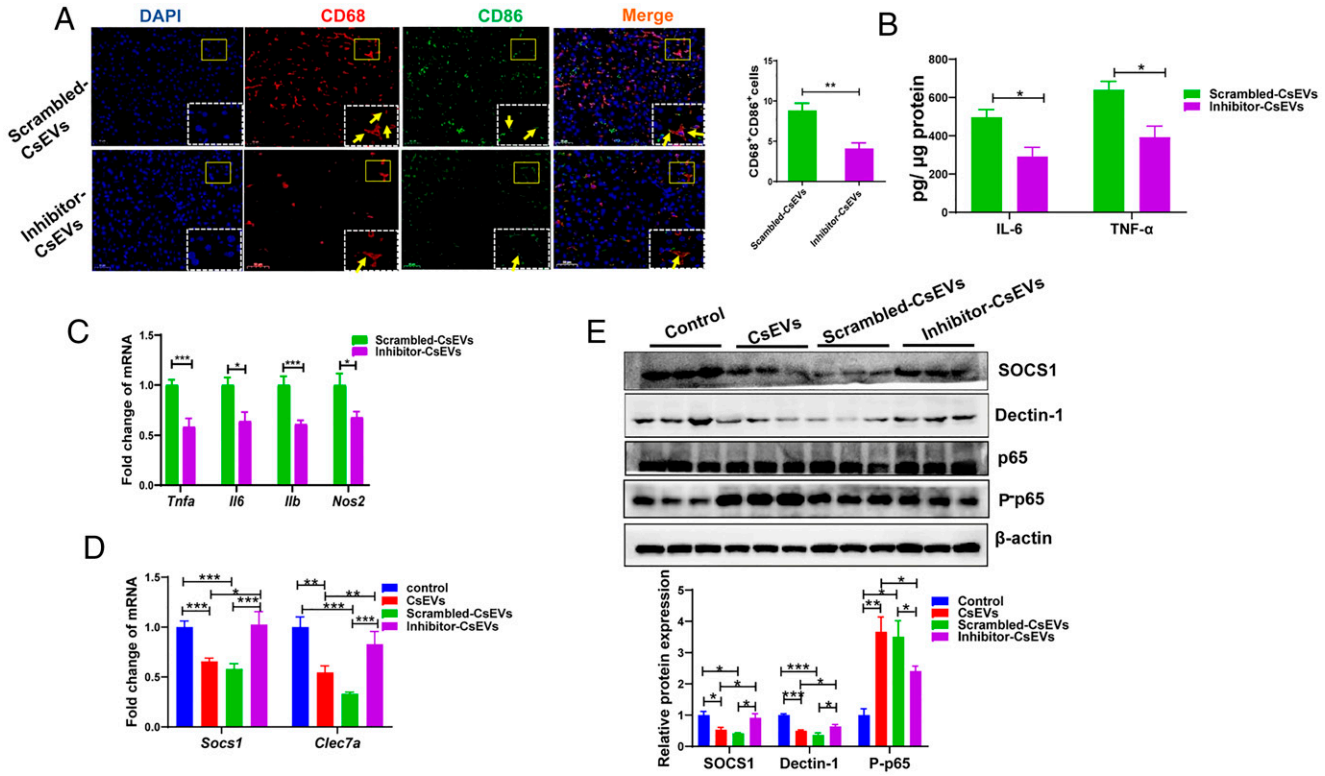

Fig. 7. Inhibition of Csi-let-7a-5p packaged by CsEVs inhibited the hepatic inflammation via targeting at SOCS1 and Dectin-1–mediated NF-κB signaling pathway. (*A*) The proportions of $CD68^{+}CD86^{+}$ macrophages (M1-like, the yellow arrows) in the livers of mice that were hydrodynamically injected (intravenouisly) with scrambled-CsEVs (0.5 mg/mL, ∼100 μL) or inhibitor-CsEVs (0.5 mg/mL, ∼100 μL) as determined by immunofluorescence assay. (*B*) ELISA data showed the production of IL-6 and TNF-α in the homogenate of liver from these mice. (*C*) The relative expression of *Tnfa*, *Il6*, *Il1b*, and *Nos2* mRNAs in the livers from these mice. (*D*) The relative expression of *Socs1* and *Clec7a* mRNAs in the liver from the mice intravenously injected with PBS (100 μL), CsEVs, scrambled-CsEVs or inhibitor-CsEVs (all 0.5 mg/mL, ∼100 μL). (*E*) The protein levels of SOCS1, Dectin-1, and P-p65 in the livers from the mice intravenously injected with PBS (100 μL), CsEVs, scrambled-CsEVs or inhibitor-CsEVs (all 0.5 mg/mL, ∼100 μL). The values were expressed as mean ± SEM. Compared with indicated groups, $*P < 0.05$, $**P < 0.01$, $***P < 0.001$.

and lipids (21). The roles of helminth-secreted EVs in the regulation of immune responses may be various due to the different types of receipt cells, the parasitic sites, and the intrinsic properties of worms. For example, several studies have shown that *S. japonicum*-derived EVs preferred M1-like macrophages that produced high levels of TNF-α (14, 22). But EVs secreted by the hookworm *Nippostrongylus brasiliensis* prevented gut inflammation by inhibition of proinflammatory cytokines (IL-6, IL-1β) (23). Little is known of *C. sinensis*-derived EVs' functions on the regulation of immune responses and the biliary damages in the condition where the worms dwell in the bile ducts for a long time and induce severe biliary injuries. In our present study, we demonstrated that CsEVs promoted activation of M1-like macrophages and induced high levels of proinflammatory cytokines (TNF-α, IL-6, IL-1β) in vitro and in vivo. These data suggested that CsEVs possessed potent abilities to induce biliary inflammation. As these inflammatory mediators played critical roles in the DRs and the damages of biliary ducts (24), we further investigated the roles of CsEVs in biliary injuries; it was found that the administration of CsEVs induced biliary hyperplasia, biliary fibrosis, and recruited massive inflammatory immune cells around biliary ducts, as well as high levels of proinflammatory cytokines (TNF-α, IL-6, IL-1β), suggesting that CsEVs induced a pro-inflammatory niche to facilitate ductal reactions. And, the data of our present study are in agreement with previous reports (24, 25).

miRNAs can be transferred by EVs a long distance to the receipt cells, as EVs provide a shuttle for miRNAs to prevent degradation during delivery. For example, hepatocyte-derived exosomal miR-192-5p actives M1 macrophages by regulation of Rictor/Akt/FoxO1 signaling in the progress of nonalcoholic fatty liver disease (26). Furthermore, different species tend to have distinct miRNA families carried in EVs (27). In the present study, we identified several miRNAs capsuled into EVs. Valadi et al. (28) showed that miRNAs of EVs were selective rather than randomly packed although the mechanisms remain unclear (29). In the present study, we found that the expression profiles of miRNAs in EVs were significantly different when it was compared with the files of miRNAs in adult worm bodies. Of these miRNAs, Csi-let-7a-5p was one of the highest enriched miRNAs in CsEVs (almost eight times), which suggested that Csi-let-7a-5p may play a role in communication between host cells and worms.

To better elucidate the roles of Csi-let-7a-5p packed by CsEVs in host–worm communication, we used Csi-let-7a-5p mimic to identify the targets and the roles in the activation of macrophages. It has been demonstrated that SOCS1 is the target of let-7-5p, and SOCS1 is a key negative regulator of NF-κB that transduced signaling to produce proinflammatory cytokines (20). Similar to these studies, we found that Csi-let-7a-5p mimic targeted at SOCS1 and inhibited the expression of SOCS1, thereby releasing the depression of NF-κB activation and promoting the expression of proinflammatory cytokines. Moreover, we also demonstrated that *Clec7a* (encoding the protein Dectin-1) was another target of Csi-let-7a-5p using a dual-luciferase activity assay. Dectin-1 is a signaling non–Toll-like receptor (TLR) pattern-recognition receptor and it has been reported that Dectin-1–mediated ERK signaling pathway

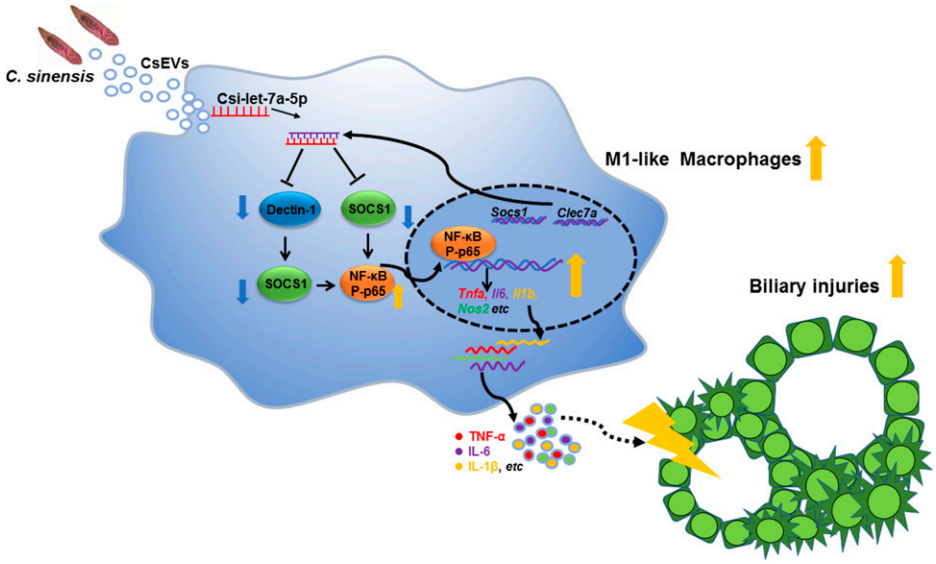

Fig. 8. A schematic model shows that Csi-let-7a-5p delivered by CsEVs from *C. sinensis* aggravates biliary injuries.

induced the expression of SOCS1 in macrophages, leading to an inhibition of NF-κB activation and the decreased transcripts of the proinflammatory cytokines (such as TNF-α and IL-6) (30, 31). In agreement with these observations, we found that Csi-let-7a-5p mimic inhibited the expression of SOCS1 and further increased the activation of NF-κB. However, let-7 showed multiple roles by targeting different genes in biliary injuries; for example, a recent study suggested that let-7 contained by EVs from liver stem cells ameliorated ductular reaction in *Mdr2*$^{-/-}$ mouse by the regulation of NF-κB and IL-13 signaling pathways (32). Another study showed that inhibition of let-7 (sponging the let-7 miRNA) by lncRNAs-H19 increased the expression of HMGA2 to enhance the proliferation of cholangiocytes and aggravate cholestatic liver injury (33). The controversy between our present observations and these studies may reflect the complex roles of let-7 in different conditions of cell types and diseases (34, 35).

RNAi has been demonstrated as an efficient and key tool for the manipulation of genes with target-specificity in the worm bodies (18, 36, 37). McVeigh et al. (18) employed RNAi to knock down *FheCatB* in Juvenile *Fasciola* spp.; they found that the transcript of *FheCatB* was silenced as early as 4 h and it can persist more than 25 d after starting soaking of double-stranded RNA. Therefore, we gene-silenced Csi-let-7a-5p in worm-bodies using siRNA via soaking and prepared CsEVs from these manipulated worms. It was found that the expression of Csi-let-7a-5p was significantly decreased both in worms and CsEVs that were treated with antisense of Csi-let-7a-5p (about 70% decreased, compared with scramble or PBS control), suggesting that Csi-let-7a-5p were successfully inhibited. Furthermore, we also observed the survival and vitality of adult *C. sinensis* cultured in the medium dynamically, it seems that the protocols used for RNAi had no potential impacts on the viability or behavior of adult *C. sinensis* (*SI Appendix*, Fig. S4), which was consistent with the observation of McVeigh et al. (18). Thus, we concluded that the decrease in the expression of Csi-let-7a-5p caused by siRNA was not due to the toxicity of siRNA to worms because the worms were still active and the eggs were persistently excreted by the worms (excreted a large number of eggs during treatment) during the whole experiment (*SI Appendix*, Fig. S4).

Consistent with the data above, the inhibitory effects of Csi-let-7a-5p on the *Clec 7a* and *Socs1* were dismissed by CsEVs with anti–Csi-let-7a-5p; accordingly, we found that CsEVs from Csi-let-7a-5p-decreased worms (Csi-let-7a-5p -inhibited CsEVs, with the aberrant Csi-let-7a-5p) significantly depressed the levels of IL-6, TNF-α, and IL-1β that were augmented by CsEVs from medium or scramble-treated worms in both in vivo and in vitro studies. Furthermore, we also confirmed that intravenous injection of Csi-let-7a-5p–inhibited CsEVs abated the biliary injuries in mice; in contrast, the biliary injuries caused by scramble-CsEVs remained unchanged, compared with those induced by normal CsEVs. Taken together, these data suggested that knockdown of Csi-let-7a-5p in CsEVs relieved the biliary inflammation and induced an amelioration of biliary injuries. However, although we found that Csi-let-7a-5p delivered by CsEVs can promote M1-like activation, it should be noted that other molecules, such as lipid-protein, long-non-coding RNAs in CsEVs, may also activate the proinflammatory phenotype of macrophages, which are not excluded.

In conclusion, our study represents a report that Csi-let-7a-5p delivered by CsEVs endows a proinflammatory hepatic microenvironment to aggravate biliary injuries by regulating *Socs1* and *Clec7a*-mediated NF-κB signaling pathway, which provides a mechanism contributing to biliary injuries caused by *C. sinensis*.

Data Availability. All of the raw data of two small RNA sequencing were deposited in the NCBI GEO, https://www.ncbi.nlm.nih.gov/geo/ (access no. GSE137695). All other study data are included in the article and *SI Appendix*.

ACKNOWLEDGMENTS. We thank Prof. Hong-Yan Dong, Zhi-Wei Liu, and Qing-Li Huang, Public Experimental Research Center, Xuzhou Medical University, for their assistance in electron microscopy analysis. This study was in part, supported by National Natural Science Foundation of China Grants 81572019, 82172297 (to K.-Y.Z.), 81702027 (to Q.Y.), and 31302077 (to C.Y.); Natural Science Foundation of Jiangsu Province of China Grants BK BK20211346 (to C.Y.) and BK20201011 (to B.-B.Z.); China Postdoctoral Science Foundation Grant 2018M640525 (to C.Y.); Qian Lan Project of Jiangsu Province (to C.Y.); Jiangsu Planned Projects for Postdoctoral Research Funds 2018K053B (to C.Y.) and RC7062005 (to B.-B.Z.); starting grants for young scientist of Xuzhou Medical University D2019040 (to B.-B.Z.); Priority Academic Program Development of Jiangsu Higher Education Institutions of China (to K.-Y.Z.); and Graduate research project of Jiangsu Province Grant KYCX20-2468 (to J.L.). The funders had no role in study design, data collection and analysis, decision to publish, or preparation of the manuscript.

1. M. B. Qian, J. Utzinger, J. Keiser, X. N. Zhou, Clonorchiasis. *Lancet* **387**, 800–810 (2016).
2. Z. L. Tang, Y. Huang, X. B. Yu, Current status and perspectives of *Clonorchis sinensis* and clonorchiasis: Epidemiology, pathogenesis, omics, prevention and control. *Infect. Dis. Poverty* **5**, 71 (2016).
3. P. Prueksapanich *et al.*, Liver fluke-associated biliary tract cancer. *Gut Liver* **12**, 236–245 (2018).
4. IARC Working Group on the Evaluation of Carcinogenic Risks to Humans, Biological agents. Volume 100 B. A review of human carcinogens. *IARC Monogr. Eval. Carcinog. Risks Hum.* **100** (Pt B), 1–441 (2012).
5. K. Sato, F. Meng, T. Giang, S. Glaser, G. Alpini, Mechanisms of cholangiocyte responses to injury. *Biochim. Biophys. Acta Mol. Basis Dis.* **1864** (4 Pt B), 1262–1269 (2018).
6. K. Sato *et al.*, Ductular reaction in liver diseases: Pathological mechanisms and translational significances. *Hepatology* **69**, 420–430 (2019).
7. S. A. MacParland *et al.*, Single cell RNA sequencing of human liver reveals distinct intrahepatic macrophage populations. *Nat. Commun.* **9**, 1–21 (2018).
8. M. E. Guicciardi *et al.*, Macrophages contribute to the pathogenesis of sclerosing cholangitis in mice. *J. Hepatol.* **69**, 676–686 (2018).
9. M. Mathieu, L. Martin-Jaular, G. Lavieu, C. Théry, Specificities of secretion and uptake of exosomes and other extracellular vesicles for cell-to-cell communication. *Nat. Cell Biol.* **21**, 9–17 (2019).
10. G. Coakley, R. M. Maizels, A. H. Buck, Exosomes and other extracellular vesicles: The new communicators in parasite infections. *Trends Parasitol.* **31**, 477–489 (2015).
11. J. S. Schorey, Y. Cheng, P. P. Singh, V. L. Smith, Exosomes and other extracellular vesicles in host-pathogen interactions. *EMBO Rep.* **16**, 24–43 (2015).
12. G. Coakley *et al.*, Extracellular vesicles from a helminth parasite suppress macrophage activation and constitute an effective vaccine for protective immunity. *Cell Rep.* **19**, 1545–1557 (2017).
13. J. F. Quintana, S. A. Babayan, A. H. Buck, Small RNAs and extracellular vesicles in filarial nematodes: From nematode development to diagnostics. *Parasite Immunol.* **39**, e12395 (2017).
14. J. Liu *et al.*, *Schistosoma japonicum* extracellular vesicle miRNA cargo regulates host macrophage functions facilitating parasitism. *PLoS Pathog.* **15**, e1007817 (2019).
15. C. Yan *et al.*, *Clonorchis sinensis* excretory/secretory products promote the secretion of TNF-alpha in the mouse intrahepatic biliary epithelial cells via Toll-like receptor 4. *Parasit. Vectors* **8**, 1–7 (2015).
16. C. Thery, S. Amigorena, G. Raposo, A. Clayton, Isolation and characterization of exosomes from cell culture supernatants and biological fluids. *Curr. Protoc. Cell. Biol.* **Chapter 3**, Unit 3.22 (2006).
17. K. Iwai, T. Minamisawa, K. Suga, Y. Yajima, K. Shiba, Isolation of human salivary extracellular vesicles by iodixanol density gradient ultracentrifugation and their characterizations. *J. Extracell. Vesicles* **5**, 30829 (2016).
18. P. McVeigh *et al.*, RNAi dynamics in Juvenile *Fasciola spp.* Liver flukes reveals the persistence of gene silencing in vitro. *PLoS Negl. Trop. Dis.* **8**, e3185 (2014).
19. F. Meng *et al.*, Functional analysis of microRNAs in human hepatocellular cancer stem cells. *J. Cell. Mol. Med.* **16**, 160–173 (2012).
20. S. Ilangumaran, R. Rottapel, Regulation of cytokine receptor signaling by SOCS1. *Immunol. Rev.* **192**, 196–211 (2003).
21. A. Marcilla *et al.*, Extracellular vesicles in parasitic diseases. *J. Extracell. Vesicles* **3**, 25040 (2014).
22. L. Wang *et al.*, Exosome-like vesicles derived by *Schistosoma japonicum* adult worms mediates M1 type immune- activity of macrophage. *Parasitol. Res.* **114**, 1865–1873 (2015).
23. R. M. Eichenberger *et al.*, Hookworm secreted extracellular vesicles interact with host cells and prevent inducible colitis in mice. *Front. Immunol.* **9**, 850 (2018).
24. C. Pinto, D. M. Giordano, L. Maroni, M. Marzioni, Role of inflammation and proinflammatory cytokines in cholangiocyte pathophysiology. *Biochim. Biophys. Acta Mol. Basis Dis.* **1864** (4 Pt B), 1270–1278 (2018).
25. J. M. Banales *et al.*, Cholangiocyte pathobiology. *Nat. Rev. Gastroenterol. Hepatol.* **16**, 269–281 (2019).
26. X. L. Liu *et al.*, Lipotoxic hepatocyte-derived exosomal microRNA 192-5p activates macrophages through Rictor/Akt/Forkhead Box transcription factor O1 signaling in nonalcoholic fatty liver disease. *Hepatology* **72**, 454–469 (2020).
27. J. Sotillo *et al.*, The protein and microRNA cargo of extracellular vesicles from parasitic helminths - current status and research priorities. *Int. J. Parasitol.* **50**, 635–645 (2020).
28. H. Valadi *et al.*, Exosome-mediated transfer of mRNAs and microRNAs is a novel mechanism of genetic exchange between cells. *Nat. Cell Biol.* **9**, 654–659 (2007).
29. J. Guduric-Fuchs *et al.*, Selective extracellular vesicle-mediated export of an overlapping set of microRNAs from multiple cell types. *BMC Genomics* **13**, 1–14 (2012).
30. M. E. Eberle, A. H. Dalpke, Dectin-1 stimulation induces suppressor of cytokine signaling 1, thereby modulating TLR signaling and T cell responses. *J. Immunol.* **188**, 5644–5654 (2012).
31. J. Ostrop, R. Lang, Contact, collaboration, and conflict: Signal integration of Syk-coupled C-type lectin receptors. *J. Immunol.* **198**, 1403–1414 (2017).
32. K. McDaniel *et al.*, Amelioration of ductular reaction by stem cell derived extracellular vesicles in MDR2 knockout mice via lethal-7 microRNA. *Hepatology* **69**, 2562–2578 (2019).
33. Y. Xiao *et al.*, Long noncoding RNA H19 contributes to cholangiocyte proliferation and cholestatic liver fibrosis in biliary atresia. *Hepatology* **70**, 1658–1673 (2019).
34. S. Jiang, Recent findings regarding let-7 in immunity. *Cancer Lett.* **434**, 130–131 (2018).
35. H. Lee, S. Han, C. S. Kwon, D. Lee, Biogenesis and regulation of the let-7 miRNAs and their functional implications. *Protein Cell* **7**, 100–113 (2016).
36. A. Anandanarayanan *et al.*, RNA interference in Fasciola gigantica: Establishing and optimization of experimental RNAi in the newly excysted juveniles of the fluke. *PLoS Negl. Trop. Dis.* **11**, e0006109 (2017).
37. B. Samarasinghe, D. P. Knox, C. Britton, Factors affecting susceptibility to RNA interference in *Haemonchus contortus* and in vivo silencing of an H11 aminopeptidase gene. *Int. J. Parasitol.* **41**, 51–59 (2011).